Reaction mechanisms of wood ash for use as a partial cement replacement

Nina M. Sigvardsen[a,*], Mette R. Geiker[b], Lisbeth M. Ottosen[a]

[a] *Department of Civil Engineering, Technical University of Denmark, Kgs. Lyngby, Denmark*

[b] *Department of Structural Engineering, Norwegian University of Science and Technology, Trondheim, Norway*

Abstract

An increase in the produced amounts of wood ashes (WAs) is seen worldwide. In this study, the potential use of two representative WAs as a partial cement replacement is investigated. The WAs originate from combustion of wood chips by grate combustion (WA1) and circulating fluidised bed combustion (WA2). Both WAs were found to possess hydraulic properties, no pozzolanic properties were detected. A substantial difference in strength development was observed between WA1 and WA2 attributed to the phases formed; WA2 contributing the most, ettringite in addition to other phases were formed, while gypsum formed in WA1 pastes.

Keywords: wood ash, hydraulic activity, pozzolanic properties, compressive strength, phase development

1. Introduction

The production of cement is responsible for 8-9% of the total anthropogenic CO_2 emissions [1]. In order to reduce the global carbon footprint, blended cements are produced, where parts of the clinker are replaced with other materials [2]. Traditionally coal fly ash from the combustion of coal has been used in blended cement, however, with the withdrawal of coal-fired power plants, a decrease in the available amounts of coal fly ash is seen. An alternative to coal biomass is used in the heating and power production, and the amount of ash originating

* Corresponding author.
E-mail address: nimasi@byg.dtu.dk (N.M. Sigvardsen).

Abbreviations (not standard): WA1: wood ash no. 1, WA2: wood ash no. 2.

from combustion of different types of biomass increases [3]. In 2018 approximately 10 million tonnes of biomass ash were produced worldwide from electricity production alone [3]. Potentially these biomass ashes could be used as mineral addition in blended cements. One of these potential mineral additions is wood ash (WA), which derived from combustion of woody products [4].

Mineral additions, traditionally used as a partial cement replacement, are divided into pozzolanic, latent hydraulic materials and (partially) inert fillers [2,5]. Pozzolanic materials, e.g. coal fly ash, form cementitious binders in reaction with calcium hydroxides. Latent hydraulic materials react with water and form cementitious binder in the presence of an activator [5]. Wood ash has varying characteristics [6,7] and varying properties when used as a partial cement replacement. Pozzolanic activity has been observed for WA in some studies [8–10] and explained by a high content of silicon, aluminium and iron oxide [9,10] or amorphous silica [8]. Lack of pozzolanic activity was found in [11,12] and explained by limited silicon content in the investigated WAs. Other studies [13–17] reported hydraulic activity for WAs reacting directly with water and forming cementitious products even without activation.

In a recent paper, Sigvardsen et al. [6] presented a multivariate data analysis linking combustion process with reaction mechanisms based on the nominative requirements to fly ash from coal combustion, as no requirements are available for the use of WA as partial cement replacement. Sigvardsen et al. [6] concluded, a WA originating from combustion of biomass (e.g. wood chips, but not limited to) from whole trees by circulating fluidised bed combustion at low temperatures is most likely to possess some pozzolanic properties, while a WA originating from grate combustion from similar biomass is most likely to possess hydraulic activity. However, results from another recent paper from Sigvardsen et al. [17] indicated that the contribution to the compressive strength development from a partial cement replacement with WA, only to a minor extent is due to pozzolanic properties and the main contribution is the hydraulic properties.

The object of this study was to test the results obtained by the multivariate analysis [6] and further investigate the results obtained by Sigvardsen et al. [17] by investigating the reaction mechanisms (pozzolanic vs hydraulic properties) of two representative WAs from the two different combustion methods; grate combustion and circulating fluidised bed combustion. Both WA originate from combustion of wood chips originating from trees, including back and needles, the most commonly used type of biofuel [18].

A report, published by representatives from Austria, Denmark, Canada, Germany, Italy and the Netherlands [3] in 2018, determined grate combustion to be predominately used combustion of biomass. Further is circulating fluidised bed combustion gaining ground in many countries, due to a high efficiency when only biomass is used as a fuel [19]. This leads to the two WAs included in this study to be of the most common type of WA produced.

2. Materials and methods

An overview of notations, including descriptions and the linked methods are provided in Tab. 1.

2.1. Materials

The fly ash fraction of two wood ashes (WAs) were used in this study; WA 1 from Skærbækværket Biomass Power Plant, Denmark and from and WA2 Värtaverket Combined Heat and Power Plant, Sweden. The two power plants use the same type of wood chips from whole trees, including bark and needle, but uses different combustion methods. Skærbækværket Biomass Power Plant uses grate combustion with combustion temperature 600-1,000°C, whereas Värtaverket Combined Heat and Power Plant use circulating fluidised bed combustion with combustion temperature 760-930°C.

WAs were collected by the staff at the power plants and transported in 50L plastic buckets. Each bucket was divided into smaller 20L buckets by taking approximate 100-200g at a time into each bucket. Subsequently, the buckets were closed and stored protected from light, heat and moist sources. Before smaller portions of WA were sampled for testing, the uniformity of the WA was increased by rotating the plastic buckets by hand.

Before use, the WAs were dried (50°C) and sieved to a particle size of ≤ 250µm. This can lead to some extent of carbonation, but it was necessary in order to obtain a controlled water content. Sieving was conducted, since the content of particles ≥ 250µm consisted only of large remnants of charred wood, accounting for ~ 25% of WA1 and less than 2% of WA2. This sieving only removed the large remnants of charred wood, thus smaller particles of charred wood can be found in the sample fraction ≤ 250µm [20].

For castings with Portland cement, Rapid Aalborg Cement (CEM I) with 5% limestone filler was used. Inert quartz (Qz) was also used for measurements of strength activity index (SAI).

87 *2.2. Methods*

88 *2.2.1. Characterisation of WAs, Qz and CEM I*

89 The content of major chemical element of the WAs, Qz and CEM I was measured on samples
90 crushed to a particle size ≤ 200µm by X-ray fluorescence (XRF) spectrometry using a
91 SPECTRO Gmbh X-LAB 2000 with a Pd-tube. Subsequently, the content of oxides could be
92 calculated from the measured element content. Loss on ignition (LoI) was measured in
93 accordance with EN 196-2 [21] and the free calcium oxides content in accordance with EN
94 451-1 [22]. Unburnt carbon content was calculated from the LoI and thermogravimetric
95 analysis (TGA) measurements.

96 pH and conductivity were measured on suspensions of WAs, Qz, and CEM I in a 2.5:1 liquid-
97 to-solid ratio in distilled water by the use of radiometer analytical electrodes after 1-hour
98 agitation. After filtration, the concentrations of water-soluble Cl^- and SO_4^{-2} were measured in
99 the filtrate by the use of Ion Chromatography (IC).

100 The particle size distribution (PSD) was determined for WAs, Qz, and CEM I by laser
101 diffraction by the use of Mastersizer 2000 and the particle density by helium gas pycnometer
102 Micrometics AccuPyc 1340 according to EN 196-6 [23].

103 X-Ray Diffraction (XRD) was used for identifying the crystalline phases in the WAs and CEM
104 I. Backloading was used to load the materials into the sample holder. For XRD measurements,
105 a PanAnalytical X-ray diffractometer sat at the PW3064 Spinner stage was used. The x-ray
106 source was Cu-Kα radiation with a wavelength of 1.54 Å. The samples were measured with a
107 step size of 0.002 °2θ and with a 24.8 s sampling time per step between 4 °2θ and 100 5 °2θ.
108 The obtained XRD plots were qualitatively evaluated by the use of X'Pert HighScore Plus
109 software, including data from the International Centre for Diffraction Data (ICDD).

110 In order to further identify and quantify phases present in the WAs and CEM,
111 thermogravimetric analysis (TGA) was performed by measuring the weight loss from room
112 temperature to 900 °C by the use of a NETZSCH STA 449 F3 Jupiter. 40 mg of the samples
113 were transferred into a 85 µl aluminium oxide crucible, and the weight loss was measured over
114 two steps: the temperature was raised to 40 °C and kept for 10 min, then increased to 900 °C
115 with a heating rate of 10 °C/min while the cell was purged with 50 ml/min of nitrogen gas. The
116 analysis software Proteus Analyzer was used for data processing.

117 *2.2.2. Determination of pozzolanic reactivity by Frattini test*

118 The pozzolanic reactivity was assessed according to EN 196-5 [24] by measuring the
119 consumption of the $Ca(OH)_2$ during curing (Frattini test). A 20g test sample, 80% CEM I and
120 20% of either of the WAs or Qz, were prepared and mixed with 100ml of distilled water. After
121 mixing, the samples were sealed in plastic bottles and left in an oven at 40°C until the test of
122 pozzolanic reactivity. The test was conducted by double determination at both 8 and 15 days.

123 Results are presented in an x/y-chart, the y-axis representing CaO [mmol/l] and the x-axis
124 representing OH^- [mmol/l]. According to EN 196-5 [24], the solubility curve of $Ca(OH)_2$ is
125 plotted over OH^- by [CaO] = 350 / ([OH]-15) for an alkaline solution at 40°C. Results plotted
126 below the solubility curve of $Ca(OH)_2$ indicates the removal of Ca^{2+} from the solution, thus
127 indicating pozzolanic activity, and results plotted above indicate saturation or oversaturation
128 with $Ca(OH)_2$ and thus no pozzolanic activity.

129 *2.2.3. Determination of pozzolanic reactivity by strength activity index (SAI)*

130 For testing of the strength activity index (SAI), mortar prisms (40 x 40 x 160mm) were cast
131 according to EN 196-1 [25]. The mix composition was 80% CEM I and 20% of either of the
132 WAs according to ASTM C311/C311M-13 [26]. For comparison, prisms with 20% cement
133 replacement by Qz and 100% CEM I was cast. The w/b was kept at 0.5, but for mixtures
134 containing either of the WAs, super plasticiser (Dynamon XTend from Mapei) were used to
135 achieve standard consistency. Consistency on the mixtures was determinate by flow table (EN
136 1015-3 [27]). The prisms were demoulded after 1 day of storage in a temperature-controlled
137 room (20°C) and subsequently stored in separate boxes for each casting (3 prisms) submerged
138 in 4.5L lime water (3g calcium hydroxide/L distilled water [28]) in a temperature-controlled
139 room (20°C) until testing. For each mix at the curing ages 7 and 28 days, three mortar prisms
140 were prepared [25].

141 SAI was measured on prisms at 7 and 28 days of curing [29]. The mortar specimens were
142 divided into two by the use of an electro-mechanic test machine (Instron 6022, 10kN) with
143 loading steps of 0.05 kN/s. The compressive strength of all six pieces of mortar sample was
144 measured for with a servohydraulic test machine (Toni Technik 300Ton) with loading steps of
145 2.4 kN/s (EN 196-1 [25]). The air content of mortars was determined from the weight at
146 demoulding, and the theoretical air void-free mortar [30] and the compressive strength was
147 normalised to an air content of 2 vol% using Bolomey's equation [31].

148 SAI was calculated from Eq. 1 [26].

$$SAI = \frac{A}{B} \quad (1)$$

149 Where:

150 A = average compressive strength of test prisms (80% CEM I + 20% WA)

151 B = average compressive strength of control prisms (100% CEM I).

152 *2.2.4. Compressive strength development of mortar with 100% WA*

153 Mortar cubes were mixed with 100% WAs as described in EN 196-1 [25], but the binder
154 content was kept constant at w/b = 0.75 and cast in 30 x 30 x 30mm silicone moulds instead
155 of as mortar prisms. The size of the mould complies with the requirements established in EN
156 12390-1 [32]. A reference mortar was cast with 100% CEM I and w/b ratio = 0.75, notated
157 REF. After 7 days of curing in the covered moulds, the cubes were demoulded and stored,
158 sealed in a box in a temperature-controlled room (20°C) until testing.

159 The compressive strength of the cubes was measured at 7, 14, 28, 60 and 90 days of curing
160 using an electro-mechanic test machine (Instron 6025, 100kN) with loading steps of 2.4 kN/s
161 [25]. All specimens were tested perpendicular to the direction of casting as a laitance layer of
162 2-3mm was seen on the reference specimens. The measured compressive strength was
163 normalised to an air content of 2 vol% as described in section 2.2.3.

164 *2.2.5. Casting and testing of 100% WA paste samples for phase development*

165 Paste samples were prepared with 100% WA with high water to binder (w/b) ratio = 0.75 in
166 order to maintain workability. A high shear mixer (Whip Mix Power Mixer Model B) was used
167 for mixing of the pastes. The mixing process was adapted from EN 196-1 [25]: mixing for 90
168 s, resting for 90 s, and mixing for 60 s. A reference was also cast with 100% CEM I and w/b
169 ratio = 0.75, notated REF. The pastes were cast in 18 ml Nalgene LDPE sample vials with snap
170 closure (diameter 27.1mm) and stored sealed in a temperature-controlled room (20°C, >90%
171 RH) until testing.

172 *2.2.5.1. Double solvent exchange*

173 For curing stoppage of the paste specimens after 7, 14, 28, 60 and 90 days of curing double
174 solvent exchange was used [33]. For each cured paste sample, four 2mm thick slices were cut

from the middle of the sample. The slices were then crushed in a porcelain mortar to a particle size of ≤ 1mm. 3g of the crushed sample was immersed in 50mL isopropanol, shaken for 30 sec, rest for 5 min and decanted. This procedure was performed twice, before the suspension was vacuum-filtered. Then the crushed sample was immersed in 10mL diethyl ether, shaken for 30sec, rest for 5 min and vacuum-filtered. After immersion in isopropanol and ether, the crushed sample was put in an oven (8 min. at 40°C) to remove remnants of the easily volatile diethyl ether [33]. Prior to further testing, the paste sample was further crushed in a porcelain mortar to a particle size of ≤ 63µm sieve [33]. The crushed paste sample was subdivided into two, and TGA and XRD analysis were conducted right away.

2.2.5.2. X-ray diffraction (XRD)

X-ray diffraction (XRD) analysis was performed on the same powdered paste samples as used for the pH and TGA, subsequent to double solvent exchange. The XRD analysis was described in section 2.2.1.

2.2.5.3. Thermogravimetric analysis (TGA)

The thermogravimetric analysis (TGA) was performed on the same powdered paste samples as used for the pH and XRD, subsequent to double solvent exchange. The TGA was described in section 2.2.1.

TGA was used to measure the loss of bound water and decomposition of portlandite, ettringite and calcite determined by the use of a horizontal step between 50°C and 550°C [34], 400°C and 550°C [34], 50°C and 120°C [35], and 600-800°C [33], respectively. The temperature interval, 50-120°C, which is used for ettringite can also include AFm phases and C-S-H [35]. This can lead to an overestimation of the precipitated ettringite. The equations (2)-(9) are used for quantification of the bound water (H), portlandite (CH), ettringite (Et) and calcite (C) content relative to the anhydrous mass binder weight (c.f. [33]).

$$H_{measured} = WL_{50-550} \tag{2}$$

$$H_{anhydrous} = \frac{H_{measured}}{weight\ at\ 550°C} \tag{3}$$

$$CH_{measured} = WL_{400-550} \cdot (74/18) \tag{4}$$

202 $$CH_{anhydrous} = \frac{CH_{measured}}{weight\ at\ 550°C} \quad (5)$$

203 $$Et_{measured} = WL_{50-120} \cdot (1255/(32 \cdot 18)) \quad (6)$$

204 $$Et_{anhydrous} = \frac{C_6As_3H_{32measured}}{weight\ at\ 550°C} \quad (7)$$

205 $$C_{measured} = WL_{600-800} \cdot (100/44) \quad (8)$$

206 $$C_{anhydrous} = \frac{C\overline{C}_{measured}}{weight\ at\ 550°C} \quad (9)$$

207

208 **3. Results**

209 *3.1 Characteristics of unreacted binders and filler (WAs, Qz and CEM I)*

210 The chemical composition of the unhydrated materials, WA1, WA2, Qz, and CEM I are
211 presented in Tab. 2 and the physical properties are presented in Tab. 3. PSD for WA1, WA2,
212 Qz, and CEM I are displayed in Fig. 1. The mean particle size were 15, 9, 24, and 13 for WA1,
213 WA2, Qz, and CEM I, respectively (Tab. 3). Fig. 2 and Tab. 4 included the crystalline phases
214 in both unhydrated WAs and CEM I. CEM I contained alite, belite, ferrite and C_3A. Both WA1
215 and WA2 contained portlandite, quartz, lime and calcite. Further WA1 contained arcanite
216 (K_2SO_4), and WA2 contains anhydrite ($CaSO_4$) and sylvite. DTG curves of unhydrated WAs
217 and CEMI are displayed in Fig. 3.

218

219 *3.2. Pozzolanic activity*

220 The Frattini test is a direct method to measure the possible pozzolanic activity of a material
221 [36], measuring the content of $Ca(OH)_2$ and its decrease as the pozzolanic reaction proceeds.
222 The result is given in Fig. 4. All results from the Frattini test are observed above the solubility
223 curve of $Ca(OH)_2$ indicating no pozzolanic activity for neither of the WAs nor the Qz.

224 The strength activity test is an indirect method used to assess the pozzolanic activity by
225 measuring a physical property [36]. The results for the investigated 20%WAs can be found in
226 Tab. 5. ASTM C618 [29] requires a strength activity index (SAI) above 0.75 for pozzolanic

materials. 20%WA1 achieved a SAI of 0.74 and 0.76, 20%WA2 achieved a SAI of 0.85 and 0.89, and 20% Qz achieved a SAI of 0.77 and 0.85 at 7 and 28 days of curing, respectively. Thus, the SAI test indicates pozzolanic activity for WA2.

3.3. Development of the compressive strength of mortar cubes with WA1, WA2 or CEM I

The development of the compressive strength of mortar cubes with either 100%WA1, 100%WA2 or plain CEM I (REF) are presented in Fig. 5. The mortar cubes with WA had at all time a lower compressive strength compared to cubes with REF. For 100%WA2, a significant increase was seen in the compressive strength rinsing from 0.6MPa at 7 days of curing to 6.4MPa at 90 days of curing, reaching 85% of the compressive strength of REF. 100%WA1 only increased in compressive strength from 0.2MPa at 7 days of curing to 1.7MPa at 90 days of curing, reaching 22% of the compressive strength of REF.

3.4. Phase development

The phase development in plain CEM I (REF), 100%WA1 and 100%WA2 pastes were analysed by XRD and TGA. The phase development in the paste specimens determined by XRD is presented in Fig. 2 and summarised in Tab. 4. For REF depletion of alite was seen after 28 days of curing. Ettringite and portlandite were seen in REF at all ages (7-90 days), in addition, increasing amounts of hemicarbonate and some monocarbonate were seen.

The hydrated 100%WA1 pastes were by XRD found to contain portlandite, quartz, calcite, potassium sulfate (arcanate) and gypsum. Lime and ettringite present in the unhydrated WA1 were note observed in the hydrated 100%WA1, while portlandite and gypsum were not found the unhydrated WA1. The hydrated 100%WA2 pastes were by XRD found to contain Portlandite, ettringite, quartz and calcite at 7 days of curing, while lime anhydrite and sylvite present in the unhydrated WA2 were not detected. At 14 days monocarbonate was detected in addition to Portlandite, ettringite, quartz and calcite. At later age (≥ 14 days), depletion of portlandite was seen. The identified phase assemblage for the 100%WAs pastes is supported by the literature [13,15].

The weight loss (DTG) curves measured by TGA confirmed the hydrate phases identified by XRD in REF: ettringite, hemicarbonate, monocarbonate and portlandite, see (Fig. 3 (a)). The

DTG curves for 100%WA2 pastes (Fig. 3 (c)) confirmed the presence of ettringite, portlandite and calcite, while the DTG curves for 100%WA1 confirmed the presence of gypsum, portlandite and calcite. In addition, a weight loss below 100ºC was observed for the hydrated pastes of both WAs (not in the unhydrated WAs). The peak appears at the decomposition temperature of, among others C-S-H and monosulfate, but the peak is sharper (the temperature interval more narrow) than expected for C-S-H, and monosulfate was not found by XRD (Fig. 4; Tab. 4), and the peak remains unidentified.

Quantification of bound water, portlandite, and calcite in the pastes, and weight loss in the temperature range 50-120 ºC calculated as ettringite are presented in Fig. 6. The weight loss between 50-120 ºC is calculated as the weight loss due to ettringite, as ettringite is considered the main contributor responsible for the set, harden and strength development of a water-WA mixture [15,37]. Three independent quantifications of the bound water, portlandite, ettringite and calcite of a reference sample (28 days of curing) are used to calculate the standard deviations; 0.67wt% for bound water, 0.56wt% for portlandite, 0.27wt% for ettringite and 0.33wt% for of calcite, displayed as error bars in Fig. 6.

A larger amount of bound water for REF was determined compared to the 100%WA pastes at all ages (Fig. 6 (a)). Further, the amount of bound water for 100%WA2 exceeded 100%WA1 at all ages, mainly due to an initial larger amount after 1 day.

Also, the amount of portlandite in REF determined by TGA exceeded the content determined in the 100%WA pastes (approximately 16 vs 5 and 1wt% after 28 days' curing). Comparing the WAs, the content of portlandite was higher for 100%WA1 than for 100%WA2 (Fig. 6 (b)).

The weight loss which is observed in the temperature range 50 - 120°C is interpreted, based on XRD, as the amount of ettringite in 100%WA2 increased notably from zero to 28 days of curing and exceeded REF at 28 days of curing (Fig. 6 (c)). No further development was observed from 28 days of curing.

Also, the 100%WA1 pastes had a weight loss in the temperature range 50 - 120°C. However, based on XRD this weight loss is not interpreted as ettringite, but attributed to the decomposition of unidentified phases. The rate of development of the phases decomposing in the temperature range 50 - 120°C was slower, and the final value lower than observed for 100%WA2. A slight increase in the amount of hydrate phases between 50 - 120°C were seen for 100%WA1 (increase 7wt%) from 7 to 60 days of curing until it became constant.

An initial increase is seen in the calcite content from unhydrated to hydrated materials which might be a result of carbonation during the double solvent exchange. The calcite content for REF was constant from 7 days of curing (Fig. 6 (d)), indicating no synergetic reaction between the limestone filler and alumina in CEM I [38]. 100%WA1 had a significantly higher calcite content compared to 100%WA2, and for both 100%WA pastes the calcite content was seen to decrease by 5-7wt% during curing (Fig. 6 (d)).

4. Discussion

The two investigated WAs included in this study originated from combustion of wood chips by grate combustion (WA1) or circulating fluidised bed combustion (WA2). As mentioned in the introduction, WAs from the two combustion processes are, based on a multivariate data analysis [6], most likely to possess hydraulic (WA1) or pozzolanic properties (WA2). Below results from the present study are summarised and discussed.

4.1. Pozzolanic properties

4.2.1 Comparison to requirements in EN 450

In order to evaluate the applicability of the WAs as a partial cement replacement, the oxide content of the WAs was assessed based on the requirements in the fly ash standard EN 450 [39]. It should, however, be noted that EN 450 [39] covers fly ash from coal combustion; thus, the assessment is only indicative. EN 450 [39] specifies requirements for the physicochemical properties for coal fly ash used in mortar and grouts. According to EN 450 [39], the sum of the content of SiO_2, Al_2O_3 and Fe_2O_3 shall not be less than 70% by mass for a pozzolanic material. None of the WAs investigated in this study meet this requirement, see Tab. 2. Thus, based solely on the oxide composition and the criteria established in EN 450 [39], a pozzolanic behaviour of WA1 and WA2 can be expected to be very limited or absent.

The pozzolanic behaviour is depending on the amount of amorphous silica and aluminosilicate present in the material [5,40]. The aluminium content was low in both WAs (1.9 and 4.9% respectively), compared to traditional coal fly ash (> 18%) [40]. Higher content of silicon was seen for WA2 compared to WA1, 21.8 versus 8.6%, but still lower than required for fly ash

coal combustion (> 32%) [40]. WA2 originates from fluidised bed combustion, where fine inert quartz of elutriated bed material is carried with the flue gas during combustion and ending in the fly ash fraction [41]. This might explain the difference in the silica content between WA1 and WA2, however, this also leads to the expectation that much of the silica in WA2 was inert.

4.2.2. Frattini test

The results of the Frattini test are displayed in Fig. 4 in accordance with EN 196-5 [24] as an x/y-chart, y-axis representing CaO [mmol/l] and x-axis representing OH^- [mmol/l], and the solubility curve of $Ca(OH)_2$. Results appearing below the solubility curve indicates removal of Ca^{2+} from the solution, attributed to pozzolanic activity, and results plotted above the solubility curve indicate oversaturation with $Ca(OH)_2$ and thus no pozzolanic activity. All tested samples (REF, 20%WA1, 20%WA2 and 20%Qz) remained saturated with portlandite over the 28 days testing period and did not show sufficient consumption of portlandite to be categorised as a pozzolan. A drawback of the Frattini test is the reliance on a) the removal of Ca^{2+} from the solution are attributed solely to the pozzolanic reactions and b) no contribution of Ca^{2+} from the mineral addition tested. This might incorrectly lead to negative results for high-Ca mineral additions which can possibly act as a source for soluble Ca^{2+} [42,43] and a false positive response in case of removal of Ca^{2+} due to precipitation of, e.g. $CaSO_4$ if extra SO_4^{2-} ions are present [43]. Based on the content of CaO > 20% in the WAs, both WAs can be categorised as high-Ca mineral additions [44] (Tab. 2), potentially contributing with soluble Ca^{2+}. Formation of gypsum was seen for WA1 and formation of ettringite was seen for WA2 (see Tab. 4.), counteracting the increased Ca^{2+} and leading to a consumption of Ca^{2+} not entailed by the pozzolanic activity. Nevertheless, based on the low content of silica and aluminosilicate potentially able to enter into pozzolanic reactions of the WAs, the results obtained from the Frattini test are considered reliable, and none of the WAs are, based on the combined chemical analysis (oxide composition of the unreacted ashes) and the Frattini test, expected to possess any significantly pozzolanic properties.

4.2.3. Strength activity index

Based on the results obtained from the SAI test (Tab. 5), WA2 appeared to possess pozzolanic properties achieving a SAI of 0.85 and 0.89 after 7 and 28 days of curing, respectively, meeting the requirements set by ASTM C618 [29] of minimum compressive strength relative to a reference sample at 0.75 after both 7 and 28 days reaction. However, so did the inert Qz, achieving a SAI of 0.77 and 0.85 after 7 and 28 days of curing. In contrast, WA1 did not possess

pozzolanic properties according to the SAI test, achieving a SAI of 0.74 and 0.76 after 7 and 28 days of curing. These results are contradictory to the results obtained by the Frattini test for WA2, and the WA2 compliance with the SAI acceptance criteria might be attributed to the WA possible possessing hydraulic properties. The positive results for Qz highlight a clear drawback of the SAI test, due to uncertainty in whether the observed strength development is actually due to pozzolanic activity or due to hydraulic properties or filler effects as expected for Qz [43,45]. Based on the relatively coarse PSD (Fig. 1), neither nucleation nor packing effects were expected for Qz. The increase in the compressive strength seen for the 20%Qz mortar might be explained by dilution of cement paste, providing more space and water for the cement reaction. Following this argument, (part of) the observed response of WA2 might also be due to a dilution effect, but as WA2 is not considered inert as Qz, this contribution is considered limited, and the contribution to the compressive strength for WA2 can be attributed to reactions between WA2, cement and water forming strength contributing hydrates. The low SAI obtained for WA1 can be explained by WA1 not acting as a filler, due to the PSD, and formation of hydrates not significantly contributing to the development of the compressive strength.

In summary, based on the low content of silica and aluminosilicate, the results from the Frattini test, and explaining the positive response of WA2 to the SAI test by hydraulic properties, none of the WAs are expected to possess any significant pozzolanic properties.

4.2. Hydraulic properties

The definition of a hydraulic binder is a binder that chemically reacts with water, facilitating a solid matrix with the ability to set and harden and, after hardening, retaining strength and stability even under water [46]. In a blended system with Portland cement (CEM I), the WAs investigated in this study retained stability even under water, but the 100% WA mortars were, when hardened, not stable in water.

4.2.1 Comparison to requirements in EN 197-1

To assess the applicability of the WAs as a partial cement replacement, the hydraulic properties of the WAs were assessed based on the requirements to oxide contents in the European cement standard EN 197-1 [46]. It should, however, be noted that EN 197-1 does currently not approve

the use of WA as a partial cement replacement, and thus the assessment is only indicative. According to EN 197-1 [46] a Portland cement clinker, defined as a hydraulic material, should comply with a CaO/SiO_2 ratio above 2 and granulated blast furnace slag, defined as a material possessing hydraulic activity when suitably activated, should comply with a $(CaO+MgO)/SiO_2$ ratio above 1. The WAs investigated in this study meet both requirements, see Tab. 2.

4.2.2 Compressive strength development

A significant difference was seen between the compressive strength development measured for the 100%WA mortar cubes and the REF mortar cubes. REF had the highest compressive strength at all ages (reaching 7 MPa after 90 days) and 100%WA1 the lowest compressive strength at all ages (see Fig. 5). 100%WA2 did not exceed the REF, but the compressive strength of 100%WA2 was increasing substantially from obtaining 10% of the compressive strength of REF at 7 days of curing to obtaining 85% of the compressive strength of REF at 90 days of curing. In comparison, 100%WA1 obtained 4% of the compressive strength of REF at 7 days of curing and 22% of the compressive strength of REF at 90 days of curing.

In summary, both investigated WAs appear to possess hydraulic properties as the 100%WA mortars were able to set, harden and develop strength, however, at a very different rate and extent and only when cured above water.

4.2.3. Phase development

The hydraulic properties of the WAs were further assessed through XRD and TGA of the reaction products formed in pastes of 100%WA. The development of crystalline phases identified by XRD is illustrated in Fig 2. and Tab. 4, summarising data for both WAs and CEM I. Based on TGA the amounts of selected phases were quantified; Fig. 6 illustrates the development with time of bound water, portlandite, calcite, and ettringite (and other phases decomposing in the temperature range 50-120°C).

Ettringite and phases decomposing in the temperature range 50-120°C

According to the literature [15,37,47,48], the formation of gypsum and ettringite are viewed as the most important phases regarding the setting and strength development of WA-water mixtures. Ettringite formation can lead to an increase in compressive strength, as a result of

411 the high content of hydrate water in ettringite increasing the hydrate volume (32 moles vs. 12
412 mole for AFm [5]), facilitating a to a reduction in the porosity [5,15]. As displayed in Fig. 6
413 (c), hydrated 100%WA2 contained a large content of ettringite, exceeding REF from 28 days
414 of curing. No ettringite was found in 100%WA1 by XRD; instead, SO_3 appeared to precipitate
415 as gypsum (Tab. 4). This is in contrast to results obtained by Sigvardsen et al. [17], where an
416 increase in the ettringite content are found in cement pastes with 10% cement replacements
417 with both WA1 or WA2. This indicates an influence of the chemistry of the cement and the
418 WAs influencing each other; the WAs contributing with an increase in the SO_3 content and the
419 cement contributing with C_3A leading to an increased SO_3/C_3A facilitating an increase in the
420 formation of ettringite [44], not seen for 100%WA pastes.

421 Ettringite precipitates when sufficient amounts of aluminium, calcium and sulfate are present
422 [50]. WA1 and WA2 have a similar total content of calcium and sulfate, thus the observed
423 difference in the ettringite content might be attributed to the difference in the alumina content;
424 1.9wt% for WA1 and 4.9wt% for WA2. This is further substantiated by the findings in
425 Sigvardsen et al. [17], where aluminium is provided by the C_3A in the cement, increasing the
426 formation of ettringite. The alumina present in WA1 appeared to precipitate as hydrogarnet, if
427 no monosulfate is considered to be present, see Fig. 3.

428 The TG curves indicate a potential presence of monosulfate (Fig. 3). However, this was not
429 confirmed by XRD and monosulphate is not stable in the presence of gypsum as it would react
430 to form ettringite [49].

431 Hemi- and monocarbonate were determined for REF (by both XRD and TGA) and
432 monocarbonate was found in 100%WA2 pastes (by XRD). Hemi- and moncarbonate
433 decompose between 60-300°C [33], which could lead to an overestimation of ettringite for REF
434 and 100%WA2 pastes, however, since the main peak lies above 120°C, this contribution is
435 considered limited.

436

437 *Portlandite*

438 Portlandite has been determined in the literature as a hydrate phase which can form during
439 curing of a WA-water mixture [15,50]. Initially, a similar content of portlandite was seen for
440 100%WA1 and 100%WA2, see Fig. 6 (b). Between 7 and 14 days of curing, a further increase
441 was seen in the portlandite content of 100%WA1, maybe due to the difference in the content

of free CaO between WA1 and WA2 (Tab. 2). At later age, the portlandite content was decreasing for both WAs.

The decrease in the portlandite content detected for 100%WA2 from 7 to 28 days of curing, corresponds to the formation of ettringite (Fig. 6 (c)). From 28 days of curing the portlandite content of 100%WA2 close to 0, corresponding to the constant content of ettringite (Fig. 6 (c)) from 28 days of curing.

The decrease in portlandite, seen for 100%WA1 from 14 to 60 days of curing, might be due to the formation of C-S-H through pozzolanic reactions as observed for other WAs by Illikainen et al. [15]. However, the amount of C-S-H precipitating as a result of pozzolanic reactions can be considered limited, both based on the TG curves (Fig. 3 b) and the results obtained by the Frattini test. Another explanation could be formation of gypsum from sulfate and portlandite, determined from 7 days of hydration by XTD (Tab. 4).

Calcite

A decrease in the calcite content was seen for both 100%WA1 and 100%WA2. The decrease in calcite for 100%WA2 is attributed to the formation of monocarbonate determined by XRD. Monocarbonate was not determined for 100%WA1, and no other phases could be identified explaining the decrease in calcite.

4.3. Comparison to the Multivariate Data Analysis and Perspectives

As previously described, Sigvardsen et al. [6] presented a multivariate data analysis investigating which types of WAs would be expected to possess hydraulic and/or pozzolanic properties based on the total content of oxides and nominative requirements. The conclusions were:

- WA originating from grate combustion of wood chips made from whole trees (in this study represented by WA1) appears as the optimal type of WA when utilised as mineral additions with hydraulic activity.
- WA originating from circulating fluidised bed combustion of biomass from whole trees at low temperatures (in this study represented by WA2) is most likely to contribute to some extent with pozzolanic properties.

From the presented study, the WAs were found to possess very limited or no pozzolanic properties and both, however, most distinguishable for WA2, possessed hydraulic properties.

The difference between the conclusions of the multivariate data analysis [6] and the observations in this study might be attributed to several reasons;

- The multivariate analysis only considered the relative amount of oxides and did not take into consideration to what extent the WAs complied with the nominative requirements established in EN 450 [39] and 197-1 [46].
- The multivariate analysis only considered the total amount of oxides not differentiating between reactive and inert parts.
- The hydraulic index included in the multivariate data analysis did not take into account the aluminium content.

Multivariate data analysis can be a powerful predicting tool, however, when assessing the possible pozzolanic or hydraulic properties of a mineral addition, the total content of oxides does not necessarily predict the actual performance. For future use of multivariate data analysis for assessing the possible use of a mineral admixture, more physicochemical characteristics of the mineral admixture need to be included, e.g. the amorphous oxide content. Furthermore, the nominative requirements need to be used with.

As a traditional pozzolanic material, WA1 and WA2 have very limited or no value. However, especially the hydraulic properties of WA2 could be advantageously utilised as a material which can be used for non-structural purposes. Further, a combination of either of the WAs with an Al-rich pozzolanic material in blended cement could increase the amount of voluminous hydrates leading to an increase in strength, thus further facilitating possible utilisation of WA in the build environment.

5. Conclusion

Two representative WAs originating from combustion of wood chips by grate combustion (WA1) and circulating fluidised bed combustion (WA2) of wood chips were investigated in this study. When mixed with water, both WAs were able to set, harden and develop strength, and thus found to possess hydraulic properties. Mortars of 100%WA2 obtained substantially more strength than mortars of 100%WA1. This was explained by a difference in the hydrate

phases, mainly gypsum was found in hydrated pastes of WA1, while ettringite was found in hydrated WA2. Neither of the WAs was categorised as a pozzolanic.

The difference in main reaction products was attributed primarily to the content of aluminium in 100%WA2, facilitating ettringite formation and the free CaO content in 100%WA1 facilitating precipitation of portlandite and subsequent formation of gypsum.

6. Acknowledgement

The Department of Civil Engineering at the Technical University of Denmark and Emineral A/S supported this work and scholarships were received from Danielsen's Foundation and EKOKEM. The plants Värtaverket Combined Heat and Power Plant (Sweden) and Skærbæk Power Plant (Denmark) are acknowledged for supplying the investigated wood ashes.

References

[1] P.J.M. Monteiro, S.A. Miller, A. Horvath, Towards sustainable concrete, Nat. Mater. 16 (2017) 698–699.

[2] B. Lothenbach, K. Scrivener, R.D. Hooton, Supplementary cementitious materials, Cem. Concr. Res. 41 (2011) 1244–1256.

[3] A.S. Frans Lamers, Marcel Cremers, Doris Matschegg, Christoph Schmidl, Kirsten Hannam, Paul Hazlett, Sebnem Madrali, Birgitte Primdal Dam, Roberta Roberto, Rob Mager, Kent Davidsson, Nicolai Bech, Hans-Joachim Feuerborn, Options for increased use of ash from biomass combustion and co-firing, IEA Bioenergy Task 32. (2018) 1–61.

[4] R. Siddique, Utilization of wood ash in concrete manufacturing, Resour. Conserv. Recycl. 67 (2012) 27–33.

[5] H. Justnes, Performance of SCMs – Chemical and Physical Principles, in: 2nd Int. Conf. Sustain. Build. Mater., 2019.

[6] N.M. Sigvardsen, G.M. Kirkelund, P.E. Jensen, M.R. Geiker, L.M. Ottosen, Impact of production parameters on physiochemical characteristics of wood ash for possible

530 utilisation in cement-based materials, Resour. Conserv. Recycl. 145 (2019) 230–240.

531 [7] I. Carević, M. Serdar, N. Štirmer, N. Ukrainczyk, Preliminary screening of wood
532 biomass ashes for partial resources replacements in cementitious materials, J. Clean.
533 Prod. 229 (2019) 1045–1064.

534 [8] R. Rajamma, R.J. Ball, L.A.C. Tarelho, G.C. Allen, J.A. Labrincha, V.M. Ferreira,
535 Characterisation and use of biomass fly ash in cement-based materials, J. Hazard. Mater.
536 172 (2009) 1049–1060.

537 [9] T. Ramos, A.M. Matos, J. Sousa-Coutinho, Mortar with wood waste ash: Mechanical
538 strength carbonation resistance and ASR expansion, Constr. Build. Mater. 49 (2013)
539 343–351.

540 [10] A.U. Elinwa, Y.A. Mahmood, Ash from timber waste as cement replacement material,
541 Cem. Concr. Compos. 24 (2002) 219–222.

542 [11] S. Demis, J.G. Tapali, V.G. Papadakis, An investigation of the effectiveness of the
543 utilization of biomass ashes as pozzolanic materials, Constr. Build. Mater. 68 (2014)
544 291–300.

545 [12] V.A. Vu, A. Cloutier, B. Bissonnette, P. Blanchet, J. Duchesne, The effect of wood ash
546 as a partial cement replacement material for making wood-cement panels, Materials
547 (Basel). 12 (2019).

548 [13] K. Ohenoja, P. Tanskanen, V. Wigren, P. Kinnunen, M. Körkkö, O. Peltosaari, J.
549 Österbacka, M. Illikainen, Self-hardening of fly ashes from a bubbling fluidized bed
550 combustion of peat, forest industry residuals, and wastes, Fuel. 165 (2016) 440–446.

551 [14] K. Ohenoja, P. Tanskanen, O. Peltosaari, V. Wigren, J. Österbacka, M. Illikainen, Effect
552 of particle size distribution on the self-hardening property of biomass-peat fly ash from
553 a bubbling fluidized bed combustion, Fuel Process. Technol. 148 (2016) 60–66.

554 [15] M. Illikainen, P. Tanskanen, P. Kinnunen, M. Körkkö, O. Peltosaari, V. Wigren, J.
555 Österbacka, B. Talling, J. Niinimäki, Reactivity and self-hardening of fly ash from the
556 fluidized bed combustion of wood and peat, Fuel. 135 (2014) 69–75.

557 [16] L. Etiégni, A.G. Campbell, Physical and chemical characteristics of wood ash,
558 Bioresour. Technol. 37 (1991) 173–178.

559 [17] N.M. Sigvardsen, M.R. Geiker, L.M. Ottosen, Phase development and mechanical
560 response of low-level cement replacements with wood ash and washed wood ash,
561 Constr. Build. Mater. 269 (2021) 121234.

562 [18] Danish Energy Agency, Energy Statistics 2018, 2018.

563 [19] R. Van Den Broek, A. Faaij, A. Van Wijk, Biomass combustion for power generation,
564 Biomass and Bioenergy. 11 (1996) 271–281.

565 [20] G.C.H. Doudart de la Grée, M.V.A. Florea, A. Keulen, H.J.H. Brouwers, Contaminated
566 biomass fly ashes - Characterization and treatment optimization for reuse as building
567 materials, Waste Manag. 49 (2016) 96–109.

568 [21] EN 196, Method of testing cement - Part 2: Chemical analysis of cement, (2013).

569 [22] EN 451, Method of testing fly ash – Part 1 : Determination of free calcium oxide content,
570 (2017).

571 [23] EN 196, Methods of testing cement – Part 6: Determination of fineness, (2018).

572 [24] EN 196, Methods of testing cement - Part 5 : Pozzolanicity test for pozzolanic cement,
573 (2011).

574 [25] EN 196, Method of testing cement - Part 1: Determination of strength, (2016).

575 [26] ASTM International C311/C311M-13, Standard Test Methods for Sampling and Testing
576 Fly Ash or Natural Pozzolans for Use in Portland-Cement Concrete., (2007) 204–212.

577 [27] EN 1015, Methods of test for mortar for masonry - Part 3: Determination of consistence
578 of fresh mortar (by flow table), (1999).

579 [28] ASTM C511-19, Standard Specification for Mixing Rooms, Moist Cabinets, Moist
580 Rooms, and Water Storage Tanks Used in the Testing of Hydraulic Cements and
581 Concretes, Am. Soc. Test. Mater. (2019) 1–3.

582 [29] ASTM International C618-15, Standard Specification for Coal Fly Ash and Raw or
583 Calcined Natural Pozzolan for Use in Concrete, (2015).

584 [30] B. Osbæck, The influence of air content by assessing the pozzolanic activity of fly ash
585 by strength testing, Cem. Concr. Res. 15 (1985) 53–64.

586 [31] G.N. Munch-Petersen, Betonhåndbogen, Dansk Betonforening, 2013.

587 [32] EN 12390, Metoder til prøvning af tilslags geometriske egenskaber – Del 1:
588 Bestemmelse af kornstørrelsesfordeling – Sigteanalyse, (2013).
589 http://findit.dtu.dk/en/catalog/2349365144 (accessed March 22, 2017).

590 [33] K. Scrivener, R. Snellings, B. Lothenbach, A Practical Guide to Microstructural
591 Analysis of Cementitious Materials, CRC Press, 2017.

592 [34] A. Machner, M. Zajac, M. Ben Haha, K.O. Kjellsen, M.R. Geiker, K. De Weerdt,
593 Portland metakaolin cement containing dolomite or limestone – Similarities and
594 differences in phase assemblage and compressive strength, Constr. Build. Mater. 157
595 (2017) 214–225.

596 [35] L. Pelletier-Chaignat, F. Winnefeld, B. Lothenbach, C.J. Müller, Beneficial use of
597 limestone filler with calcium sulphoaluminate cement, Constr. Build. Mater. 26 (2012)
598 619–627.

599 [36] S. Donatello, M. Tyrer, C.R. Cheeseman, Comparison of test methods to assess
600 pozzolanic activity, Cem. Concr. Compos. 32 (2010) 121–127.

601 [37] I. Odler, K.-H. Zysk, Hydraulic Properties of Fluidized Bed Combustion Ashes, MRS
602 Proc. 178 (1989) 189.

603 [38] K. De Weerdt, K.O. Kjellsen, E. Sellevold, H. Justnes, Synergy between fly ash and
604 limestone powder in ternary cements, Cem. Concr. Compos. 33 (2011) 30–38.

605 [39] EN 450, Fly ash for concrete - Part 1: Definition, specifications and conformity criteria,
606 (2012).

607 [40] M. Thomas, Supplementary Cementing Materials in Concrete, CRC Press, 2013.
608 https://www.taylorfrancis.com/books/9781466573017 (accessed April 24, 2020).

609 [41] S. van Loo, J. Koppejan, The Handbook of Biomass Combustion and Co-firing, Taylor
610 & Francis Ltd, 2010.

611 [42] R. Snellings, K.L. Scrivener, Rapid screening tests for supplementary cementitious
612 materials: past and future, Mater. Struct. Constr. 49 (2016) 3265–3279.

613 [43] S. Donatello, A. Freeman-Pask, M. Tyrer, C.R. Cheeseman, Effect of milling and acid
614 washing on the pozzolanic activity of incinerator sewage sludge ash, Cem. Concr.
615 Compos. 32 (2010) 54–61.

616 [44] P. Barnes, J. Bensted, Structure and Performance of Cements, 2nd ed., Taylor & Francis,
617 London and New York, 2002.

618 [45] S. Ramanathan, H. Moon, M. Croly, C. Chung, P. Suraneni, Predicting the degree of
619 reaction of supplementary cementitious materials in cementitious pastes using a
620 pozzolanic test, Constr. Build. Mater. 204 (2019) 621–630.

621 [46] EN 197, Cement - Part 1: Composition, specifications and conformity criteria for
622 common cements, (2011).

623 [47] E.J. Anthony, E.M. Bulewicz, K. Dudek, A. Kozak, The long term behaviour of CFBC
624 ash-water systems, Waste Manag. 22 (2002) 99–111.

625 [48] X.G. Li, Q. Bin Chen, K.Z. Huang, B.G. Ma, B. Wu, Cementitious properties and
626 hydration mechanism of circulating fluidized bed combustion (CFBC) desulfurization
627 ashes, Constr. Build. Mater. 36 (2012) 182–187.

628 [49] F. Winnefeld, B. Lothenbach, Phase equilibria in the system Ca 4 Al 6 O 12 SO 4–Ca 2
629 SiO 4–CaSO 4–H 2 O referring to the hydration of calcium sulfoaluminate cements,
630 RILEM Tech. Lett. 1 (2016) 10–16.

631 [50] B.M. Steenari, L.G. Karlsson, O. Lindqvist, Evaluation of the leaching characteristics
632 of wood ash and the influence of ash agglomeration, Biomass and Bioenergy. 16 (1999)
633 119–136.

634

635 **Table 1.** Overview of methods and notations.

	Property/ Method	WA1	WA2	Qz	CEM I			
Unhy-drated	Elemental composition	x	x		x			
	Particle size distribution	x	x	x	x			
	LoI	x	x		x			
	Free CaO	x	x					
		100% WA1	100% WA2	100% Qz	REF	20% WA1	20% WA2	20% Qz
Hydrated	Strength activity index on mortar prims				x	x	x	x
	Frattini test on WA in water				x	x	x	x
	Compressive strength on mortar cubes	x	x	x	x			
	Phase development (TGA, XRD) on paste samples	x	x	x	x			

636

637 **Table 2.** Chemical composition (%) of unreacted WA1, WA2, Qz and CEM I. ± indicates the standard deviation.

	WA1	**WA2**	**Qz**	**CEM I**

SiO_2	8.6	21.8	99.4	19.7
Al_2O_3	1.9	4.9	0.10	5.4
Fe_2O_3	2.3	2.7	0.03	3.8
CaO	48.9	45.2	0	64.1
MgO	3.8	4.0	0	1.0
K_2O	16.8	7.2	0	0.4
Na_2O	2.2	0.8	0	0.3
SO_3	5.4	5.8	0	3.2
$SiO_2 + Al_2O_3 + Fe_2O_3$	12.9	29.4	0	-
CaO / SiO_2	5.7	2.1	-	-
$(CaO + MgO) / SiO_2$	6.1	2.3	-	-
Cl^-	0.8 ± 0.0	0.4 ± 0.0	0.0 ± 0.0	0.0 ± 0.0
SO_4^{-2}	3.8 ± 0.0	1.8 ± 0.0	0.0 ± 0.0	0.0 ± 0.0
LoI, 950ºC	15.0 ± 0.1	16.2 ± 0.3	0.0 ± 0.0	1.9 ± 0.0
Unburnt carbon	≥ 1.0	5.7	-	-
Free CaO	12.3 ± 0.7	6.4 ± 0.2	-	-

Table 3. Physical characteristics of unreacted WA1, WA2, Qz and CEM I. ± indicates the standard deviation.

	WA1	**WA2**	**Qz**	**CEM I**
pH	13.0 ± 0.1	12.7 ± 0.1	7.7 ± 0.1	12.8 ± 0.0
Mean particle size (D50)	15 ± 0.5	9 ± 0.2	24.6 ± 0.4	13 ± 0.1
Particle density (kg/m^3)	2740	2710	2650	3180

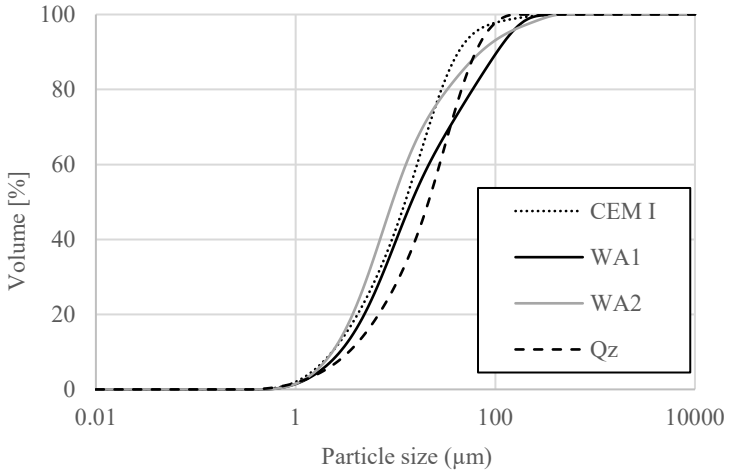

Figure 1. Particle size distribution of unreacted CEMI, WA1, WA2 and Qz, determined by laser diffraction.

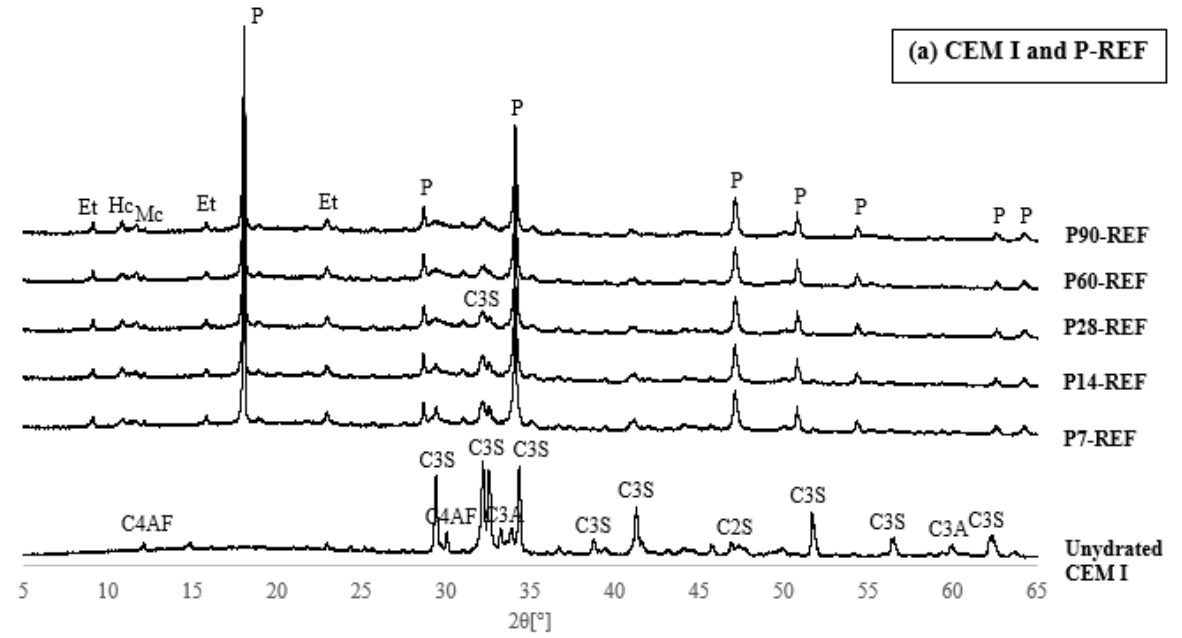
(a) CEM I and P-REF
P90-REF
P60-REF
P28-REF
P14-REF
P7-REF
Unydrated CEM I
Et Hc Mc Et Et
C4AF
C3S
C2S
C3A
2θ[°]

643

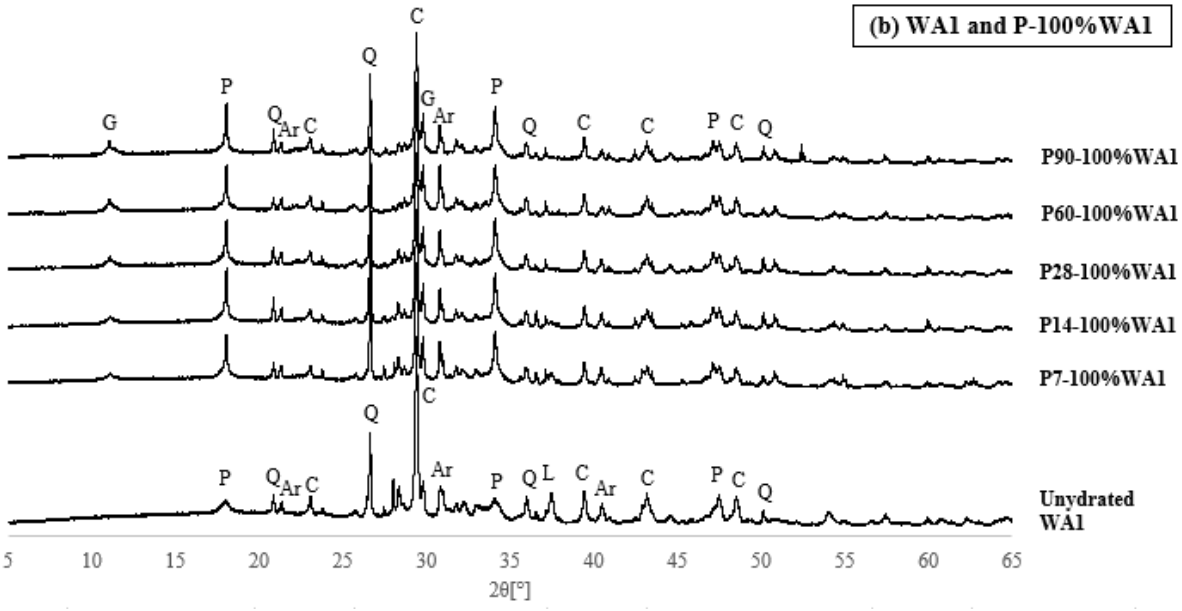
(b) WA1 and P-100%WA1
P90-100%WA1
P60-100%WA1
P28-100%WA1
P14-100%WA1
P7-100%WA1
Unydrated WA1
G P Q Ar C
L
2θ[°]

644

645

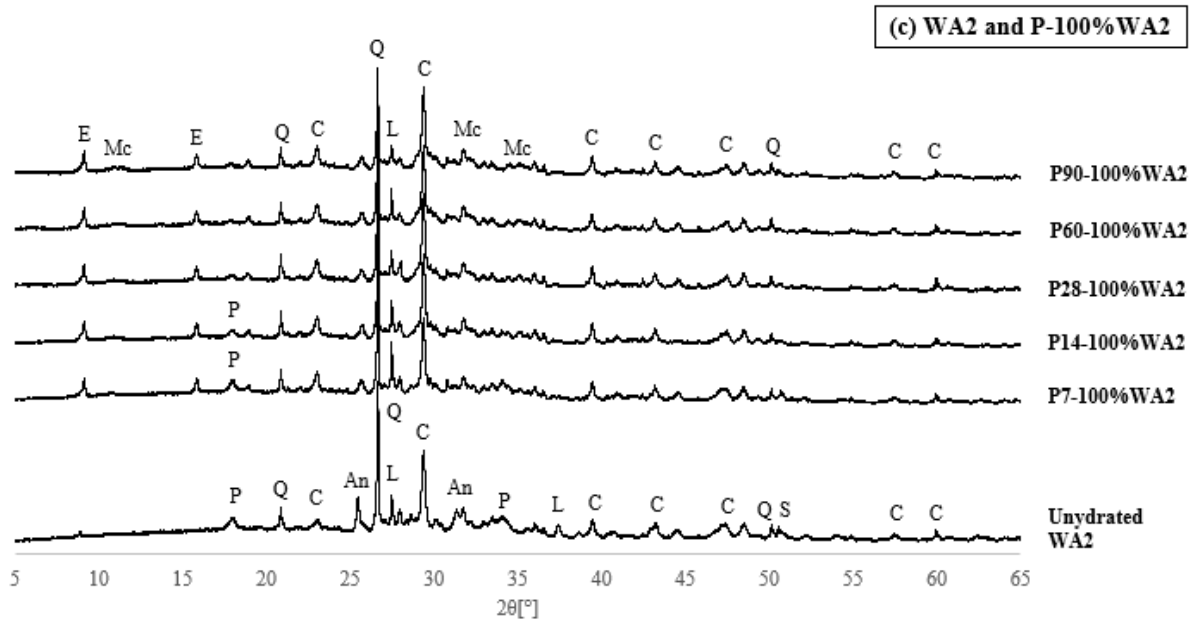

Figure 2. XRD patterns between 5 °2θ and 65 °2θ for the unreacted materials and hydrated pastes, (a) Unhydrated CEMI and cured REF pastes, (b) Unhydrated WA2 and cured 100%WA1 pastes and (c) Unhydrated WA2 and cured 100%WA2 pastes. Et: Ettringite, Hc: Hemicarbonate, Mc: Monocarbonate, P: Portlandite, G: Gypsum, Ar: Arcanite, C: Calcite, L: Lime, An: Anhydrite, S: Sylvite.

Table 4. Crystalline phases for unhydrated CEM I, WA1 and WA2, and for 100%WA1, 100%WA2 and REF paste samples investigated after 7, 14, 28, 60 and 90 days of curing at 20°C determined qualitatively by XRD diffraction.

	Alite	Belite-β	Ferrite	C_3A	Lime (CaO)	Arcanite (K_2SO_4)	Anhydrite ($CaSO_4$)	Sylvite (KCl)	Portlandite	Ettringite	Quartz	Calcite	Monocarbonate	Hemicarbonate	Gypsum ($CaSO_4{\cdot}2(H_2O)$)
Unhydrated CEM I	x	x	x	x											
Unhydrated WA1					x	x				x	x	x			
Unhydrated WA2					x		x	x		x	x	x			
P7-REF	x								x	x					
P7-100%WA1						x			x		x	x			x
P7-100%WA2									x	x	x	x			
P14-REF	x								x	x			x	x	
P14-100%WA1						x			x		x	x			x
P14-100%WA2									x	x	x	x	x		
P28-REF	x								x	x			x	x	
P28-100%WA1						x			x		x	x			x
P28-100%WA2										x	x	x	x		
P60-REF									x	x			x	x	
P60-100%WA1						x			x		x	x			x
P60-100%WA2										x	x	x	x		
P90-REF									x	x			x	x	
P90-100%WA1						x			x		x	x			x

P90-100%WA2			x	x	x	x

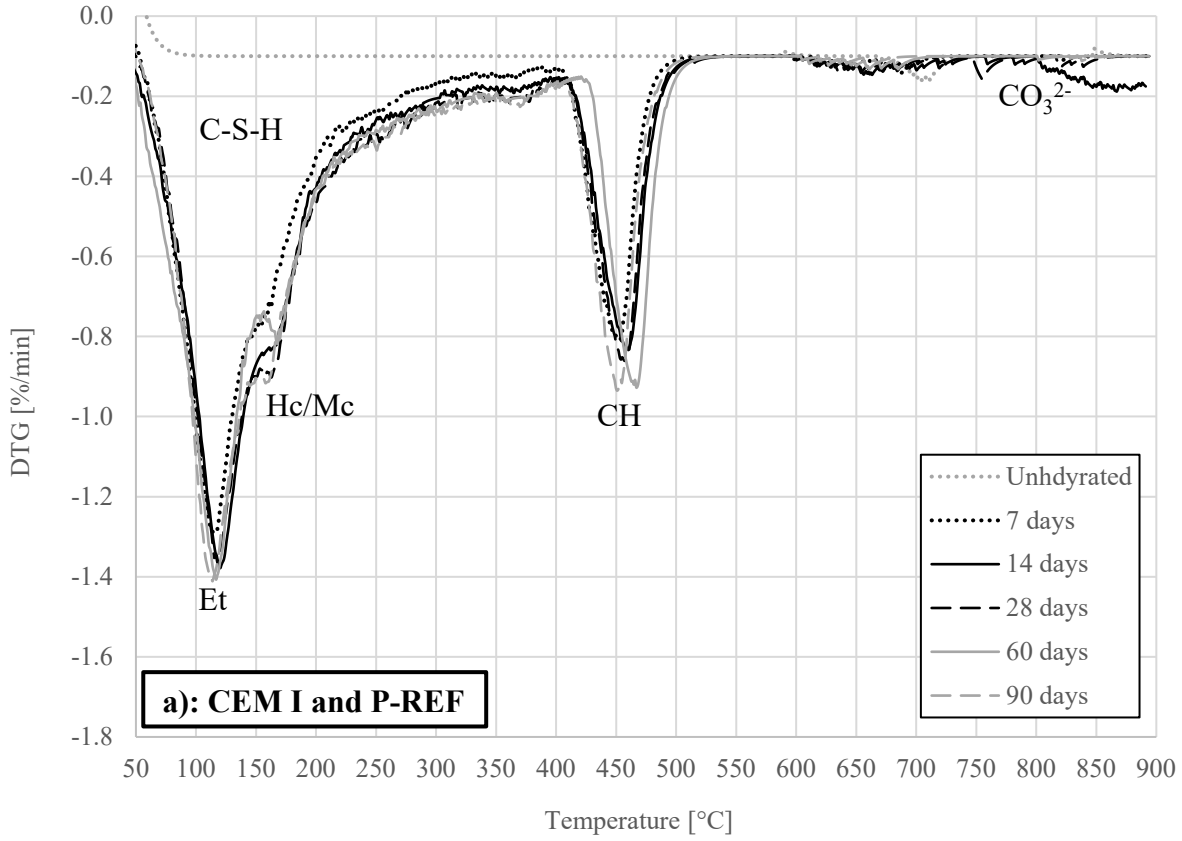

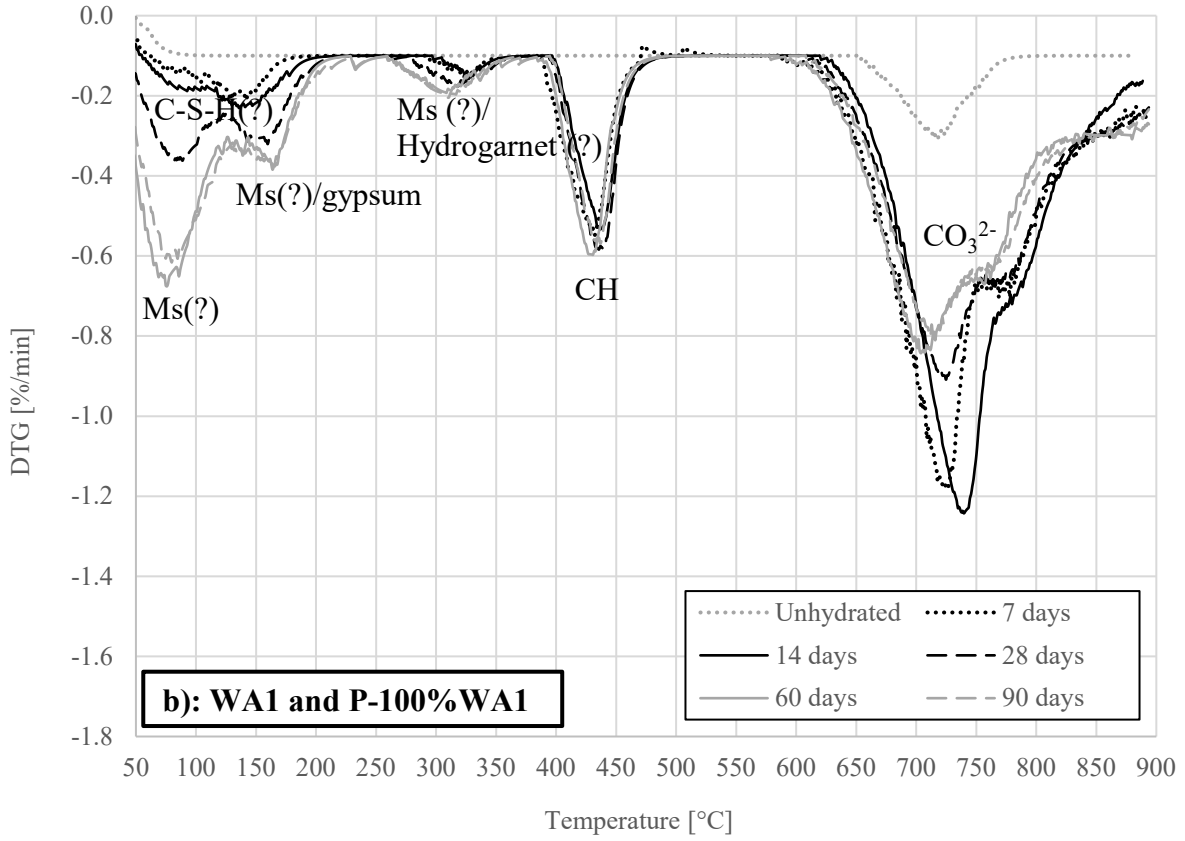

661

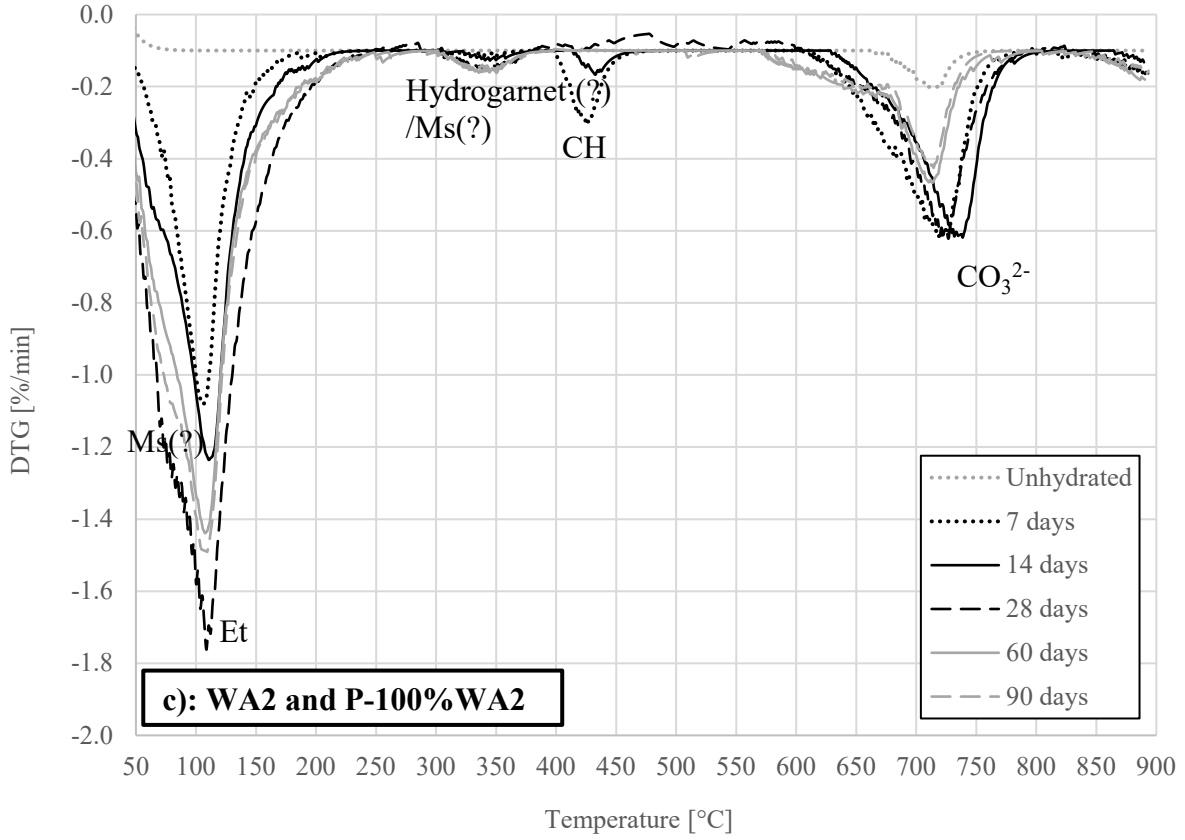

662

663 **Figure 3.** DTG curves of unhydrated and hydrated CEM I, WA1 and WA2 paste samples. (a) Unhydrated CEMI
664 and cured REF pastes, (b) Unhydrated WA2 and cured 100%WA1 pastes and (c) Unhydrated WA2 and cured

100%WA2 pastes at 7, 14, 28, 60, and 90 days of curing. C-S-H: Calcium-silicate-hydrate, Mc: Monocarbonate, Hc: Hemicarbonate, Et: Ettringite, CH: portlandige, Ms: Monosulfate.

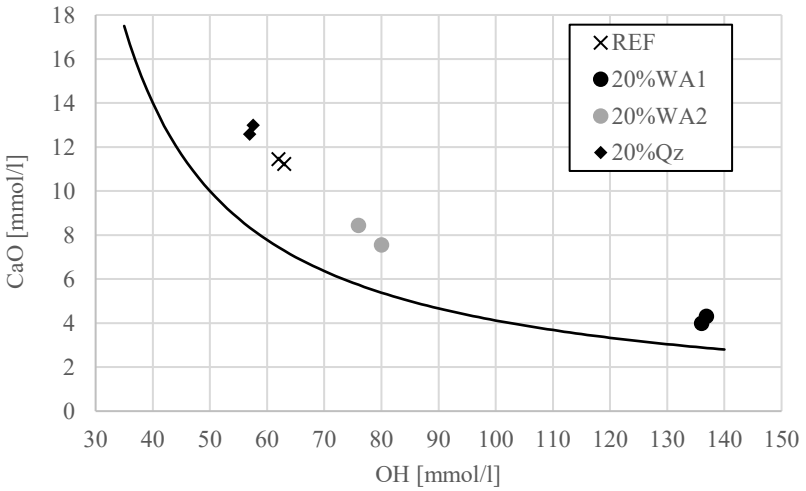

Figure 4. Frattini test results for a reference mixture and three mixtures with 20% replacement of CEM I with WA1, WA2 and Qz, respectively.

Table 5. Measured compressive strength for 20%WA1, 20%WA2, 20%Qz and REF mortar prims, air content, compressive strength normalised to an air content of 2 vol% and calculated SAI.

	Compressive strength (MPa)	SD	Air content (%vol)	Normalised compressive strength (MPPa)	Strength activity index (SAI)
M7-REF	60	3.6	1.1	58	-
M7-20%WA1	44	0.7	1.0	43	0.74
M7-20%WA2	50	0.7	1.0	49	0.85
M7-20%Qz	46	0.9	1.0	44	0.77
M28-REF	70	1.8	1.1	65	-
M28-20%WA1	51	1.3	1.0	49	0.76
M28-20%WA2	59	1.4	1.0	57	0.89
M28-20%Qz	57	1.4	1.0	55	0.85

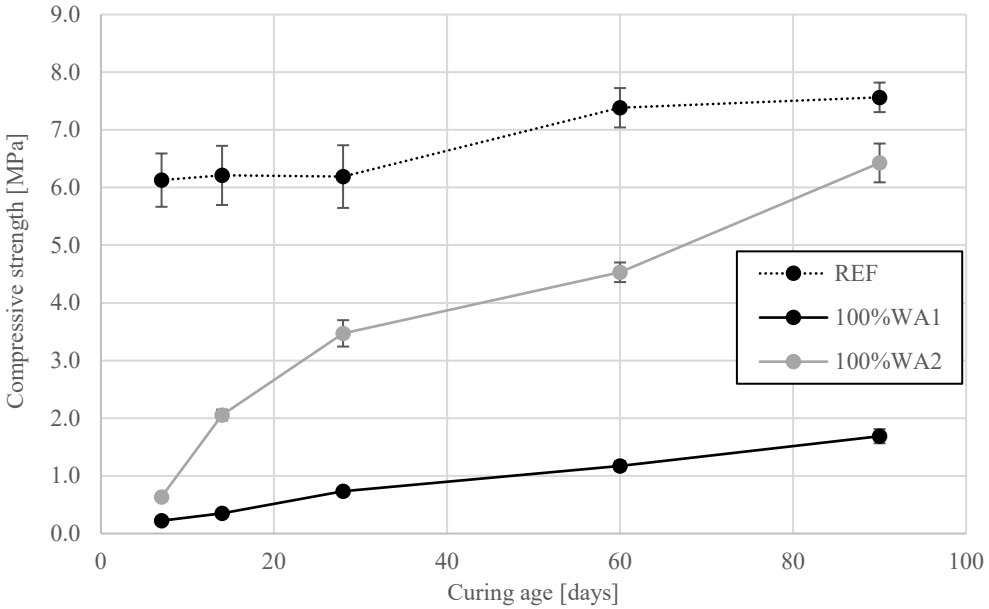

Figure 5. Compressive strength for 100%WA1, 100%WA2 and REF mortar cubes investigated after 7, 14, 28, 60 and 90 days of curing at 20°C. The compressive strength normalised to an air content of 2 vol% by the use of Bolomeys equation [31]. The error bars indicates the standard deviation.

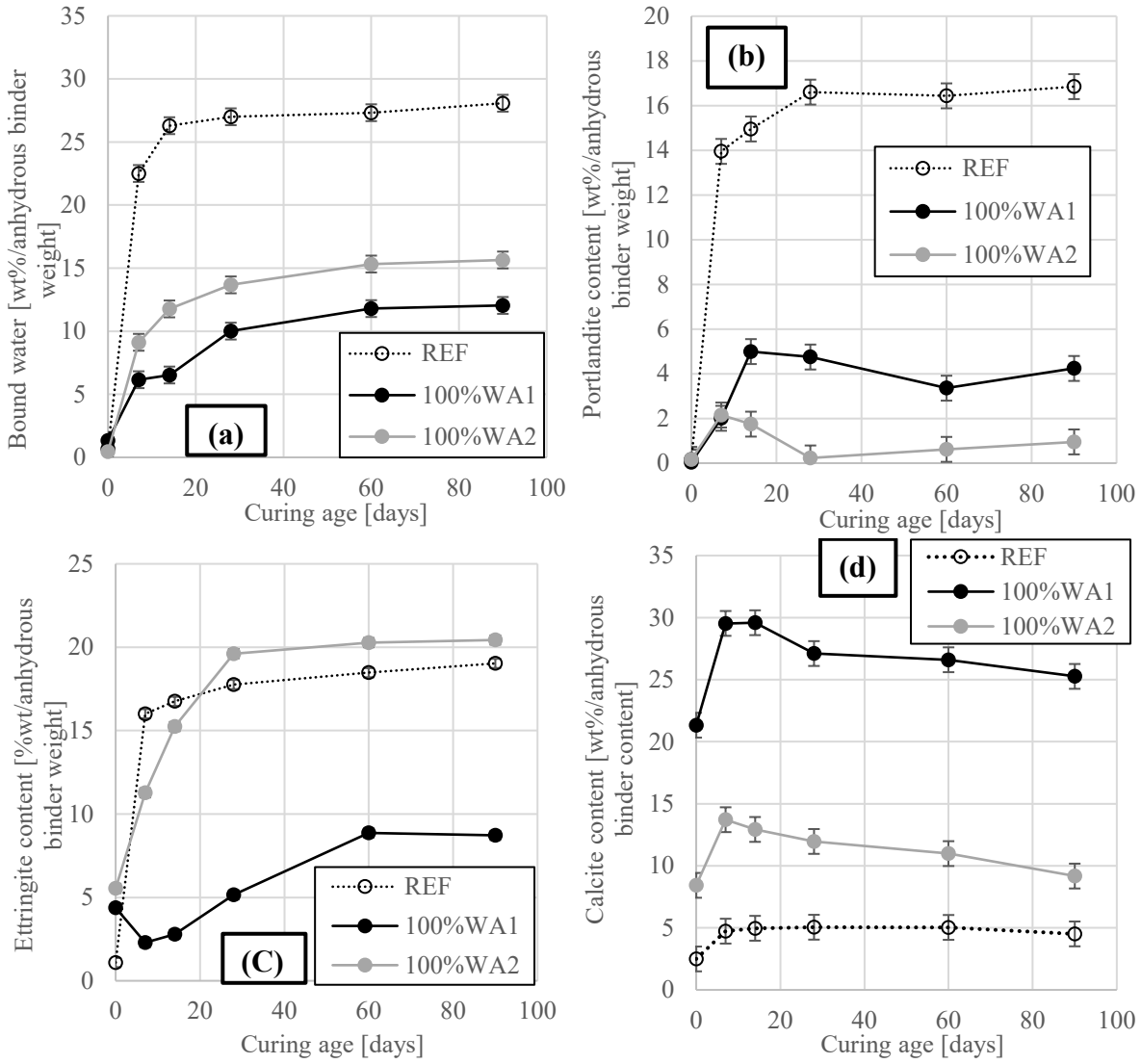

687
688 **Figure 6.** Quantification of bound water (a), portlandite (b), ettringite (c) and calcite (d) normalised to anhydrous
689 binder for 100%WA1, 100%WA2 and 100% CEM I paste samples investigated after 7, 14, 28, 60 and 90 days of
690 curing at 20°C. Unhydrated 100%WA1, 100%WA2 and CEM I are included as 0. The error bars indicates the
691 standard deviation.